Journal of Hazardous Materials 180 (2010) 71–78

Contents lists available at ScienceDirect

Journal of Hazardous Materials

journal homepage: www.elsevier.com/locate/jhazmat

Sub-grid scale combustion models for large eddy simulation of unsteady premixed flame propagation around obstacles

Valeria Di Sarli[a,*], Almerinda Di Benedetto[a], Gennaro Russo[b]

[a] Istituto di Ricerche sulla Combustione, Consiglio Nazionale delle Ricerche (CNR), Via Diocleziano 328, 80124, Naples, Italy
[b] Dipartimento di Ingegneria Chimica, Università degli Studi di Napoli Federico II, Piazzale Tecchio 80, 80125, Naples, Italy

ARTICLE INFO

Article history:
Received 14 August 2009
Received in revised form 1 March 2010
Accepted 3 March 2010
Available online 9 March 2010

Keywords:
Large eddy simulation
Unsteady flame propagation
Premixed combustion
Obstacles
Sub-grid scale combustion models

ABSTRACT

In this work, an assessment of different sub-grid scale (sgs) combustion models proposed for large eddy simulation (LES) of steady turbulent premixed combustion (Colin et al., Phys. Fluids 12 (2000) 1843–1863; Flohr and Pitsch, Proc. CTR Summer Program, 2000, pp. 61–82; Kim and Menon, Combust. Sci. Technol. 160 (2000) 119–150; Charlette et al., Combust. Flame 131 (2002) 159–180; Pitsch and Duchamp de Lageneste, Proc. Combust. Inst. 29 (2002) 2001–2008) was performed to identify the model that best predicts unsteady flame propagation in gas explosions. Numerical results were compared to the experimental data by Patel et al. (Proc. Combust. Inst. 29 (2002) 1849–1854) for premixed deflagrating flame in a vented chamber in the presence of three sequential obstacles. It is found that all sgs combustion models are able to reproduce qualitatively the experiment in terms of step of flame acceleration and deceleration around each obstacle, and shape of the propagating flame. Without adjusting any constants and parameters, the sgs model by Charlette et al. also provides satisfactory quantitative predictions for flame speed and pressure peak. Conversely, the sgs combustion models other than Charlette et al. give correct predictions only after an *ad hoc* tuning of constants and parameters.

1. Introduction

Modeling premixed flame propagation in gas explosions is a difficult task given that explosions are intrinsically unsteady phenomena, with flames transiting through different combustion regimes [1,2].

When the flame starts propagating away from an ignition source, a weak turbulence, which is not able to affect the flame propagation, develops. From this, the increasing turbulence level, induced by the interaction between the moving flame and obstacles in its path, allows the vortices formed ahead of the flame front to wrinkle the flame, increasing its surface area. Eventually, the vortices can also enter the flame structure, increasing the transport of heat and mass in the preheating zone (and thus the flame thickness) or disrupting/quenching the flame either locally or globally.

To capture the transient flame-vortex interaction is the key step when modeling gas explosions.

Thanks to the growing computational power and the availability of parallel computing algorithms, large eddy simulation (LES) is becoming a standard tool to model turbulent combustion. The attraction of LES is that it offers an improved representation of turbulence, and the resulting flame-turbulence interaction, with respect to classical Reynolds-averaged Navier–Stokes (RANS) models.

LES explicitly resolves the large turbulent structures in a flow field (up to the grid dimension), modeling the small structures that, however, exhibit a more "universal" behavior. Unfortunately, chemical reactions in combustion processes occur at characteristic scales that are generally smaller than the affordable mesh resolution. Thus, combustion has to be modeled at the sub-grid level.

In LES of turbulent premixed combustion, the flame front is too thin to be resolved on the computational grid. To overcome this obstacle, three main approaches have been proposed based on an artificially thickened flame (TF) concept, a flame front tracking technique (G-equation) and a flame surface density (FSD) description [3,4]. In all cases, sub-grid scale (sgs) models are needed to take into account the effect of the small vortices on the combustion rate (the effect of the large vortices on the flame surface area is directly simulated in LES).

The choice of the sgs combustion model is the crucial point for LES of unsteady premixed flame propagation in explosions. It is important to identify combustion models able to quantify the coupling between sub-grid turbulence and reaction rate in each combustion regime, and also to capture the transition between regimes. In addition, these models should provide quantitative predictions with minimal dependence on constants and parameters.

So far, great effort has been devoted to the development and validation of sgs combustion models for LES of steady turbulent

* Corresponding author. Tel.: +39 0817622673; fax: +39 0817622915.
E-mail address: valeria.disarli@irc.cnr.it (V. Di Sarli).

0304-3894/$ – see front matter © 2010 Elsevier B.V. All rights reserved.
doi:10.1016/j.jhazmat.2010.03.006

Nomenclature

a	constant
A	constant
b_1	constant
b_3	constant
c	reaction progress variable
c_{ms}	constant (≈ 0.28)
c_v	constant
C_k	Kolmogorov constant (≈ 0.15)
d	exponent
D	diffusion coefficient
Da_Δ	sub-grid scale Damköhler number
f	function
f_{Re}	function
f_u	function
f_Δ	function
Ka	Karlovitz number
Pr	Prandtl number
Re_t	turbulent Reynolds number
Re_Δ	sub-grid scale Reynolds number
Sc_Δ	sub-grid scale Schmidt number
S_L	laminar burning velocity
S_L^*	local burning velocity of the *broadened* flame [11]
t	time
u	velocity
u'_Δ	sub-grid scale turbulent velocity
w	local burning velocity
Y_f	local fuel mass fraction
Y_f^o	fuel mass fraction in the unburned mixture

Greek symbols

β	parameter
γ	parameter
Γ	efficiency function
δ_F	laminar flame thickness
Δ	filter size
ν	kinematic viscosity
Ξ_Δ	sub-grid scale flame wrinkling factor
ρ	fluid density
ρ_0	density of the unburned gas
Σ	sub-grid scale flame surface density
$\dot{\omega}_c$	reaction rate

premixed combustion, such as that encountered in combustors and burners (see, e.g., [5–18]). It has been demonstrated that these models are able to take into account the flame-turbulence interaction in fully developed turbulent combustion regimes. However, it is still unclear whether they are fit for transient combustion phenomena such as explosions.

All LES models proposed for premixed flame deflagration in the presence of obstacles are based on the FSD approach [19–24]. It has been shown that the identification of the combustion regimes through which the flame propagation evolves (ranging from the laminar regime up to the *thin reaction zones* regime) is consistent with the *flamelet* assumption on which such an approach relies [20,22].

In most of the works by Masri's group [19–21], the algebraic closure for the sgs flame surface density by Boger et al. [5] was used. Although this sgs combustion model exhibits a weak dependence of the combustion rate on the unresolved vortices, the results obtained show good predictions in terms of flame position, structure and interactions with flow and turbulence. The discrepancies observed with regard to the pressure trend have been attributed to the sgs combustion model. Ibrahim et al. [24] obtained more accurate predictions using the dynamic FSD formulation by Knikker et al. [15].

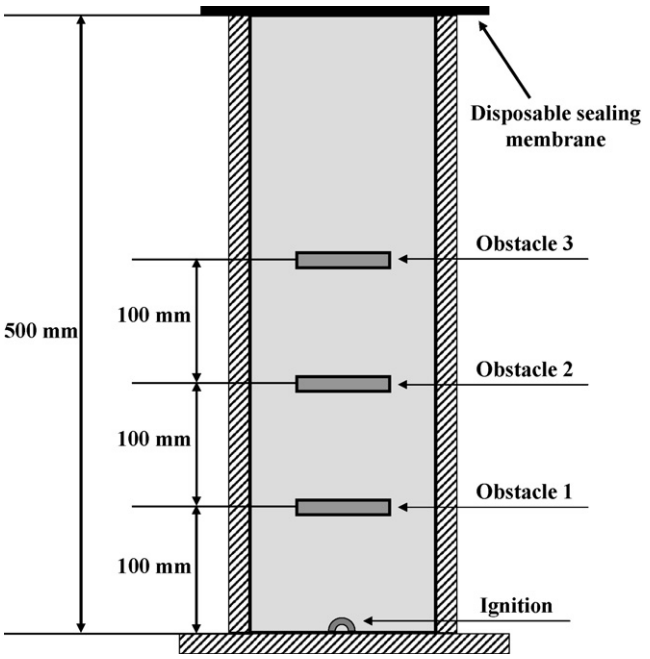

Fig. 1. Schematic diagram of the explosion chamber by Patel et al. [25].

In our papers [22,23], the power-law flame wrinkling model by Charlette et al. [12] was used and a satisfactory agreement with experimental data has been found (shape of the propagating flame, flame speed, pressure peak, velocity vector fields). Large eddy simulations were also run with the effect of the sgs combustion model eliminated, thus separating the role of the large (resolved) vortices from that of the small (sgs) vortices [22]. The results obtained demonstrate that the large scale vortices play the dominant role in dictating all trends, including the development of the flame structure along the path. Conversely, the sgs vortices do not affect the qualitative trends. However, it is essential to model their effect on the combustion rate to achieve reliable predictions for both flame speed and pressure peak.

In the present work, large eddy simulations of unsteady premixed flame propagation around three sequential obstacles in a vented chamber were carried out for different sgs combustion models. More precisely, we tested five sgs models developed for steady turbulent combustion [9–13]. These sgs models significantly differ in quantifying the strength of the combustion–turbulence interaction.

Numerical results were compared to experimental data with the aim at identifying the sgs combustion model that best predicts unsteady flame propagation with no tuning of constants and parameters used in the model itself.

2. Test case

Simulations were run of the experiment by Patel et al. [25]. A schematic diagram of the explosion chamber used for the experiment is presented in Fig. 1. The chamber was a 150 mm × 150 mm × 500 mm volume constructed from polycarbonate to provide optical access. Three obstacles (150 mm × 75 mm × 12 mm) were positioned at 100-mm spacings within the chamber. The bottom end of the chamber was closed. The upper end was sealed by a thin PVC membrane whose rupture during the combustion process allowed the burned gases to escape.

The set-up at the exit of the chamber was essentially an air gap followed by a fume extraction system.

A stoichiometric mixture of methane and air was purged through the chamber and ignited at the center of the closed end starting from rest. The presence of multiple obstacles in the flame path allowed the flame to achieve a wide range of combustion regimes [22,25].

The experiment provided highly resolved data for model validation. A high-speed laser-sheet flow visualization (HSLSFV) system was employed to image the flame propagation at an image recording rate of 9000 Hz. From the high-speed video sequence, the flame speed as a function of the axial distance from the ignition face was also derived. The speed was calculated as the displacement of the maximum downstream location of the flame front.

The pressure time history was taken from recordings obtained using a high-speed piezoelectric pressure transducer located close to the point of ignition.

The experiment demonstrated a high level of reproducibility with flame shapes and speeds being directly comparable between different combustion events. However, there was a slight variation in the time taken for the flame to reach the first obstacle of ±0.5 ms. This variation, which was maintained throughout the combustion process, can be attributed to the time taken for early flame kernel development. As a result of this repeatability in combustion behavior, the pressure traces demonstrated little deviations between events other than the temporal shift of ±0.5 ms with respect to ignition.

3. Model description

The large eddy simulation (LES) model used in this work has been described previously [22].

The model equations were obtained applying a Favre-filter (i.e., a mass-weighted filter) to the Navier–Stokes equations for conservation of mass, momentum, energy and chemical species, coupled to the constitutive and state equations.

The species transport equation was recast in the form of a transport equation for the reaction progress variable, c, which is zero within fresh reactants and unity within burned products [26]:

$$c = 1 - \frac{Y_f}{Y_f^o} \tag{1}$$

In Eq. (1), Y_f is the local fuel mass fraction and Y_f^o is the fuel mass fraction in the unburned mixture. The conservation equation for c reads as follows:

$$\frac{\partial \rho c}{\partial t} + \nabla \cdot (\rho u c) = \nabla \cdot (\rho D \nabla c) + \dot{\omega}_c \tag{2}$$

In Eq. (2), the two left-hand side terms correspond respectively to unsteady effects and convective fluxes, while the two right-hand side terms correspond to molecular diffusion and reaction rate.

The filtering process filters out the turbulent structures whose scales are smaller than the filter width so that the resulting equations govern the dynamics of the large scale structures. However, owing to the non-linear nature of the conservation equations, the filtering operation gives rise to unknown terms that have to be modeled at the sub-grid scale (sgs) level [3].

The unknown terms arising from the momentum equation and the energy equation are the sgs stress tensor and the sgs heat flux, respectively.

The LES Favre-filtered c-equation can be written as:

$$\frac{\partial \bar{\rho} \widetilde{c}}{\partial t} + \nabla \cdot \left(\bar{\rho} \widetilde{u} \widetilde{c}\right) + \nabla \cdot \left[\bar{\rho} \left(\widetilde{uc} - \widetilde{u}\widetilde{c}\right)\right] = \overline{\nabla \cdot (\rho D \nabla c)} + \bar{\dot{\omega}}_c \tag{3}$$

where the overbar $(-)$ denotes a filtered quantity and the tilde $(\sim)$ a Favre-filtered quantity. In Eq. (3), there are three unknown terms: the sgs reaction progress variable flux (third term on the left-hand side), the sgs molecular diffusion (first term on the right-hand side) and the sgs reaction rate (second term on the right-hand side).

3.1. Sub-grid scale (sgs) closures for stress tensor and scalar fluxes

The closure of the sgs stress tensor was achieved with the dynamic Smagorinsky-Lilly eddy viscosity model [27]. The model coefficient was dynamically calculated during the LES computations using the information about the local instantaneous flow conditions provided by the smallest scales of the resolved (known) field. This allowed the resulting eddy viscosity to respond properly to the local flow structures.

The sgs fluxes of heat and reaction progress variable were modeled through the gradient hypothesis [3]. The sgs turbulent Prandtl and Schmidt numbers were assumed to be constant and equal to 0.7 [28].

3.2. Sub-grid scale (sgs) combustion models

Among the different approaches proposed to handle the flame-turbulence interaction in LES [3], the flame surface density (FSD) formalism based on the *flamelet* concept was here chosen. The main assumption in *flamelet* models is that of a "thin flame sheet", which means that the flame, or at least the reaction zone, is thinner than the smallest turbulent scale (i.e., the Kolmogorov scale), thus remaining laminar. Furthermore, the high gradients within the thin flame allow a balance to be established between molecular transport and chemical reactions. This implies that diffusive transport and chemistry cannot be modeled independently of each other. Accordingly, the two filtered terms of molecular diffusion and reaction rate (right-hand side terms in Eq. (3)) were included in a single term, $\overline{\rho w \left|\nabla c\right|}$, expressed as:

$$\overline{\rho w \left|\nabla c\right|} = \overline{\nabla \cdot (\rho D \nabla c)} + \bar{\dot{\omega}}_c = \left\langle \rho w \right\rangle_S \Sigma \tag{4}$$

where Σ is the sgs flame surface density (i.e., the sgs flame surface per unit volume) and $\left\langle \rho w \right\rangle_S$ is the surface-averaged mass-weighted combustion rate per unit flame surface.

In Eq. (4), $\left\langle \rho w \right\rangle_S$ was approximated by $\rho_0 S_L$ [29], where ρ_0 is the fresh gas density and S_L is the laminar burning velocity. Σ was expressed as a function of the sgs flame wrinkling factor, Ξ_Δ, (i.e., the sgs flame surface divided by the projection of the flame surface in the propagating direction):

$$\overline{\rho w \left|\nabla c\right|} = \left\langle \rho w \right\rangle_S \Sigma = \rho_0 S_L \Xi_\Delta \left|\nabla \bar{c}\right| \tag{5}$$

In Eq. (5), Ξ_Δ takes into account the effects of interaction between flame propagation and unresolved sgs turbulence.

In the present work, an assessment of different sgs combustion models proposed for LES of steady turbulent premixed combustion was performed [9–13]. The model by Kim and Menon [11] was coupled to the dynamic kinetic energy model for the sgs stress tensor [30].

The sgs combustion models tested differ on the basis of the formula for calculating Ξ_Δ (Table 1).

Fig. 2 shows the sgs wrinkling factor, Ξ_Δ, as a function of the Karlovitz number, i.e., the ratio of the chemical time to the time of the Kolmogorov scale, Ka $(= [(u'_\Delta/S_L)^3 \times (\delta_f/\Delta)]^{1/2})$, for different combustion models. The values of constants and parameters used in each model are those suggested by the authors (Table 1). The x-axis of the figure covers the range of interest (Ka = 0–10) for the various stages of flame propagation within the chamber [22]. These Ka values fall within the limit of validity of the *flamelet* assumption made

Table 1
Formula of the sgs wrinkling factor, Ξ_Δ, for each combustion model tested.

Sgs combustion model	Formula for the wrinkling factor, Ξ_Δ	Constants and parameters
Colin et al. [9]	$\Xi_\Delta = 1 + \beta \frac{2\ln(2)}{3c_{ms}(Re_t^{1/2}-1)} \Gamma\left(\frac{\Delta}{\delta_F}, \frac{u'_\Delta}{S_L}\right) \frac{u'_\Delta}{S_L}$	$\beta = 1$
	with $\Gamma\left(\frac{\Delta}{\delta_F}, \frac{u'_\Delta}{S_L}\right) = 0.75 \exp\left[-\frac{1.2}{(u'_\Delta/S_L)^{0.3}}\right] \left(\frac{\Delta}{\delta_F}\right)^{2/3}$	
Flohr and Pitsch [10]	$\Xi_\Delta = 1 + a(Re_\Delta Pr)^{1/2} Da_\Delta^{-1/4}$	$a = 0.52$
Kim and Menon [11]	$\Xi_\Delta^\gamma = \left(\frac{S_L^*}{S_L}\right)^\gamma + \beta \left[\frac{u'_\Delta}{S_L}\left(1 - \left(\frac{Av}{Pr\Delta S_L}\frac{S_L^*}{S_L}\right)^{2/3}\right)^{1/2}\right]^\gamma$	$\beta = 1$; $\gamma = 2$; $A = 6$; $c_v = 0.05$
	with $\frac{S_L^*}{S_L} = f\left(1.5^{1.2} c_v \left(\frac{\Delta}{Pr}\frac{u'_\Delta}{S_L}\right)^{4/3} Re_\Delta^{-1/3}\right)$	
Charlette et al. [12]	$\Xi_\Delta = \left(1 + \min\left[\frac{\Delta}{\delta_F}, \Gamma\left(\frac{\Delta}{\delta_F}, \frac{u'_\Delta}{S_L}, Re_\Delta\right)\frac{u'_\Delta}{S_L}\right]\right)^\beta$	$\beta = 0.5$
	with $\Gamma\left(\frac{\Delta}{\delta_F}, \frac{u'_\Delta}{S_L}, Re_\Delta\right) = \left[\left(\left(f_u^{-d} + f_\Delta^{-d}\right)^{-1/d}\right)^{-1.4} + f_{Re}^{-1.4}\right]^{-1/1.4}$	
	where $f_u = 4\left(\frac{27C_k}{110}\right)^{1/2}\left(\frac{18C_k}{55}\right)\left(\frac{u'_\Delta}{S_L}\right)^2$	
	$f_\Delta = \left[\frac{27C_k\pi^{4/3}}{110} \times \left(\left(\frac{\Delta}{\delta_F}\right)^{4/3} - 1\right)\right]^{1/2}$	
	$f_{Re} = \left[\frac{9}{55}\exp\left(-\frac{3}{2}C_k\pi^{4/3}Re_\Delta^{-1}\right)\right]^{1/2} \times Re_\Delta^{1/2}$	
	$d = 0.6 + 0.2\exp\left(-0.1\frac{u'_\Delta}{S_L}\right) - 0.2\exp\left(-0.01\frac{\Delta}{\delta_F}\right)$	
Pitsch and Duchamp de Lageneste [13]	$\Xi_\Delta = 1 + \frac{u'_\Delta}{S_L} b_3 \left[\left(\mathrm{Da}_\Delta/\mathrm{Sc}_\Delta\right) / \left(1 + \frac{b_3^2}{b_1^2 \mathrm{Sc}_\Delta}\mathrm{Da}_\Delta\right)\right]^{1/2}$	$b_1 = 2$; $b_3 = 1$

in the approach adopted to model the flame-turbulence interaction [3].

All sgs models recover the laminar burning velocity (i.e., $\Xi_\Delta = 1$) in regions of low turbulence activity. However, compared to the other sgs models, Colin et al. [9] predicts much lower wrinkling factors. Conversely, Pitsch and Duchamp de Lageneste [13] predicts much higher wrinkling factors. Charlette et al. [12], Kim and Menon [11] and Flohr and Pitsch [10] are between these two extreme behaviors.

The differences in the trends of Fig. 2 have to be attributed to the domain of validity of each sgs combustion model.

The sgs models by Colin et al. [9] and Charlette et al. [12] were specifically developed for LES, starting from direct numerical simulation (DNS) of elementary flame-vortex interactions. An efficiency function, Γ, was introduced which takes into account the net wrinkling effect of all relevant turbulent scales smaller than the filter size, Δ (Table 1). In both models, Γ was constructed from a spectral analysis of DNS data. However, two different approaches were chosen for such kind of analysis. Furthermore, in Charlette et al. [12], Γ was corrected such that the eddies whose characteristic speed falls below $S_L/2$ (very slow eddies) do not wrinkle the flame.

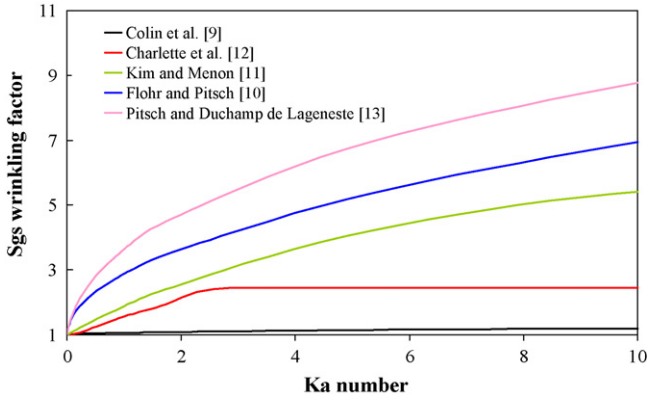

Fig. 2. Sgs wrinkling factor *versus* the Ka number for different combustion models.

Charlette et al. [12] implemented the sgs combustion model in an LES code in the context of the thickened flame (TF) approach, and performed simulations of a premixed flame embedded in a time-decaying isotropic turbulence in several different parameter ranges. They also ran direct numerical simulations and successfully compared LES and DNS results in terms of total reaction rate. In addition, comparisons between the predicted overall turbulent burning velocity as a function of the root mean square velocity and the experimental data by Abdel-Gayed and Bradley [31] showed a close agreement over a significant range of parameters, which also overshoots the *corrugated flamelets* regime.

The domains of validity for the sgs combustion models by Flohr and Pitsch [10], Kim and Menon [11] and Pitsch and Duchamp de Lageneste [13] range up to the *thin reaction zones* regime.

Flohr and Pitsch [10] and Pitsch and Duchamp de Lageneste [13] extended to LES the RANS models by Zimont and Lipatnikov [32] and Peters [33], respectively.

Kim and Menon [11] combined their *broadened* flame model with the two flame wrinkling models by Pocheau [34] and Yakhot [35]. Both formulations were implemented in an LES code based on the G-equation method to simulate premixed flame propagation in a realistic gas turbine combustor. Numerical predictions were compared to experimental data on mean and fluctuating spatial velocity profiles. The best agreement was obtained with Pocheau's formulation that was tested in this work (Table 1).

3.3. Numerics

The model equations were discretized using a finite volume formulation on a tri-dimensional non-uniform structured grid. The grid-independence of the solution was checked for each sgs com-

Table 2
Total CPU time for each sgs combustion model tested.

Sgs combustion model	Total CPU time [s]	Relative additional total CPU time [%]
Colin et al. [9]	903	12.6
Flohr and Pitsch [10]	869	8.3
Kim and Menon [11]	996	24.2
Charlette et al. [12]	862	7.5
Pitsch and Duchamp de Lageneste [13]	872	8.7
No sgs combustion model (i.e., $\Xi_\Delta = 1$ in Eq. (5))	802	–

bustion model. The results presented in Section 4 were obtained employing the same grid (the finest grid) in all simulations. This choice was motivated by the need to compare the performances of the sgs combustion models keeping constant the ratio of resolved to unresolved turbulence. The grid was composed of around 930,000 hexahedral cells, with minimum and maximum resolutions equal to 2 and 3 mm, respectively. Smaller cell size (2 mm) was used close to the walls owing to the presence of steeper gradients of the solution field.

For the spatial discretization of the model equations, second order bounded central schemes were chosen. The time integration was performed using the second order implicit Crank-Nicholson scheme.

Adiabatic and no-slip wall boundary conditions were applied at the solid interfaces (bottom and vertical faces of the chamber, faces of the obstacles). To calculate the shear stress at the wall, a blended linear/logarithmic law-of-the-wall was used [36].

Outside the combustion chamber, the computational domain was extended to include a dump vessel. A condition of fixed static pressure ($=1.013 \times 10^5$ Pa) was specified at the boundaries of this additional domain whose volume (1650 mm × 1650 mm × 750 mm) allowed minimizing the interference between the reflected pressure waves and the pressure field inside the chamber.

Initial conditions had velocity components, energy and reaction progress variable set to zero everywhere. Ignition was obtained by means of a hemispherical patch, with a radius equal to 5 mm, of hot combustion products at the centre of the closed end of the chamber.

The specific heats of the unburned and burned mixtures were approximated as piecewise fifth-power polynomial functions of temperature. The molecular viscosities were calculated according to Sutherland's law for air viscosity. The laminar burning velocity was assumed to be constant with pressure and temperature and equal to 0.41 m/s [37,38].

Computations were performed by means of the segregated solver of the Fluent code (version 6.3.26) [39] employing the SIMPLE method to treat the pressure-velocity coupling. The code was parallelized on a 64-bit computing Beowulf cluster consisting of 3 dual-CPU nodes (6 processors) each of them being an AMD Opteron 260 with 2 GB of RAM. The solution for each time step required around 20 iterations to converge with the residual of each equation smaller than 6×10^{-4}.

Concerning the computing performances of the sgs combustion models, the values of the total CPU time (on 6 parallel processors) needed by each model for a single time step are given in Table 2.

It is worth saying that the CPU time depends on the flame surface area (i.e., on the number of grid cells where there is active combustion) and, thus, varies during the computations. The values reported in Table 2 were calculated at the time instant when the flame reaches the first obstacle and starts interacting with the turbulence induced at the obstacle wake. In these conditions, the flame surface area is substantially the same regardless of the sgs combustion model implemented (the transition from laminar to turbulent flame propagation is starting to take place).

The time needed without any sgs combustion model (i.e., assuming $\Xi_\Delta = 1$ in Eq. (5)) is also given in Table 2 along with the relative additional time for each model. It can be seen that Kim and Menon [11] has an additional time of 24.2% which is about two times higher than the additional time of Colin et al. [9], and three times higher than the additional time of Charlette et al. [12], Flohr and Pitsch [10] and Pitsch and Duchamp de Lageneste [13].

4. Results and discussion

4.1. Comparison of the sub-grid scale (sgs) combustion models

The numerical predictions obtained using the sgs combustion models [9–13] with the original values of constants and parameters (i.e., the values suggested by the authors, Table 1) are here compared to the experimental data by Patel et al. [25] in order to evaluate the predictive capability of the models.

In Fig. 3, the LES and experimental flame speed profiles along the axial distance from the ignition face are shown.

All sgs models are able to reproduce qualitatively the experimental trend with the steps of flame acceleration and deceleration around the obstacles (the black rectangles in Fig. 3 indicate the positions of the obstacles). However, only the sgs model by Charlette et al. [12] provides results that are in quantitative agreement with the experimental data. Among the sgs models other than Charlette et al., Colin et al. [9] predicts flame speeds lower than the experimental ones. On the contrary, the sgs models by Kim and Menon [11], Flohr and Pitsch [10] and Pitsch and Duchamp de Lageneste [13] overpredict the flame speed.

Fig. 4 shows the pressure time histories calculated for different sgs combustion models, together with the experimental trend.

The sgs model by Colin et al. [9] underpredicts the pressure peak that appears much weaker and later than in the experiment. Conversely, Kim and Menon [11], Flohr and Pitsch [10] and Pitsch and Duchamp de Lageneste [13] simulate stronger and earlier peaks. The sgs model by Charlette et al. [12] provides the best quantitative prediction of the pressure peak which, as in the experiment, is found at about 37 ms after ignition. However, also this sgs model underestimates the maximum pressure (the maximum overpres-

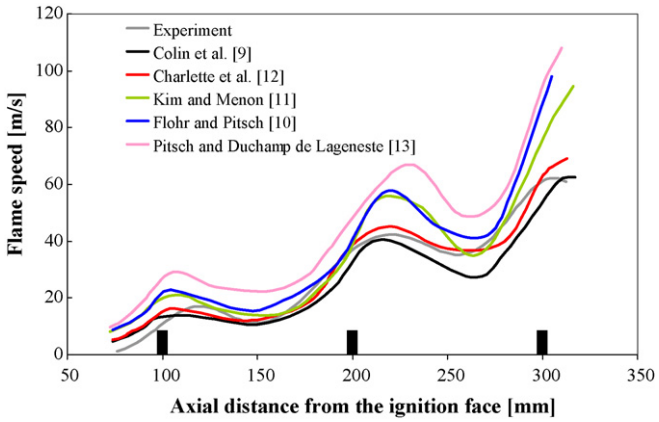

Fig. 3. Flame speed *versus* the axial distance from the ignition face: experimental data by Patel et al. [25] and LES results for different sgs combustion models.

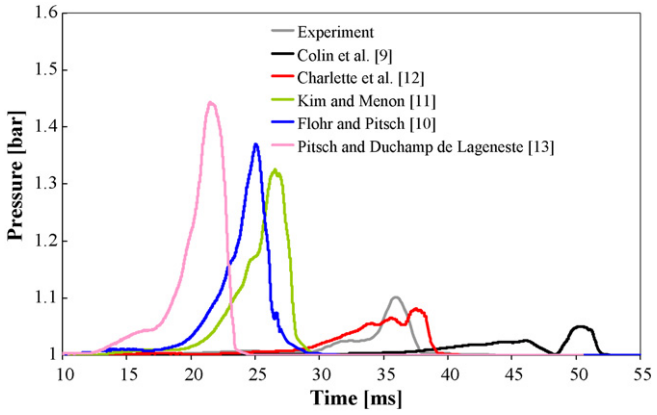

Fig. 4. Pressure time history at the bottom end of the explosion chamber: experimental data by Patel et al. [25] and LES results for different sgs combustion models.

sure is around 20% lower than the experimental value). This can be attributed to the fact that the effect of the PVC membrane was not simulated.

Figs. 3 and 4 reflect the dependence of the sgs wrinkling factor on the Karlovitz (Ka) number and, thus, on the unresolved turbulence of the models (Fig. 2). Colin et al. [9], which exhibits very weak dependence, simulates the slowest flame propagation and the weakest pressure peak. On the contrary, Pitsch and Duchamp de Lageneste [13], which exhibits very strong dependence, gives rise to the fastest flame propagation and the most severe pressure peak.

In Fig. 5, the field profiles of the sgs combustion rate ($= \rho_0 S_l \Xi_\Delta \left|\nabla \tilde{c}\right|$) are shown as obtained with (a) Colin et al. [9], (b) Charlette et al. [12] and (c) Pitsch and Duchamp de Lageneste [13]. These profiles were taken at the time instants (also reported in Fig. 5) when the flame exits the chamber.

As would be expected, the lowest sgs combustion rate is observed with Colin et al. [9], the highest with Pitsch and Duchamp de Lageneste [13]. However, whatever the sgs model, the flame shape is substantially the same as found in the experiment by Patel et al. [25]. The vortical structures induced behind the obstacles wrinkle the flame and also disrupt the continuity of the front, giving rise to the formation of flame pockets. With Pitsch and Duchamp de Lageneste [13], the higher turbulence level associated to the flame propagation leads to an early breakdown of the flame front at the wake of the first obstacle.

It is worth saying that Patel et al. [25] also ran unsteady RANS (URANS) simulations of their experiment. The comparison with the results obtained here demonstrates that the LES approach overcomes the difficulties of URANS in capturing the acceleration and deceleration of the flame around the obstacles as well as relevant features of the flame shape and structure (asymmetric shape, wrinkling of the flame front, pocket formation).

4.2. Adjusted sub-grid scale (sgs) combustion models

From the above comparisons, it is clear that the sgs combustion model by Charlette et al. [12] provides good agreement with the experimental data, both qualitatively and quantitatively. The sgs models other than Charlette et al. [9–11,13] are all able to capture the qualitative trends. However, they result in worse quantitative predictions for flame speed and pressure peak.

On the other hand, the differences among the sgs combustion models tested are quantitative in simulating the strength of the interaction between flame and turbulence (Fig. 2). LES computations were then run using values of constants and parameters in the sgs models [9–11,13] different from those listed in Table 1. The original values were modified (see Table 3) in order to obtain trends of the sgs wrinkling factor *versus* the Ka number as close as possible to the trend by Charlette et al. [12].

In Fig. 6, the sgs wrinkling factors are plotted *versus* the Ka number, as obtained assuming for all models the *adjusted* values of constants and parameters given in Table 3. The trends for these *adjusted* sgs models match the trend by Charlette et al. [12].

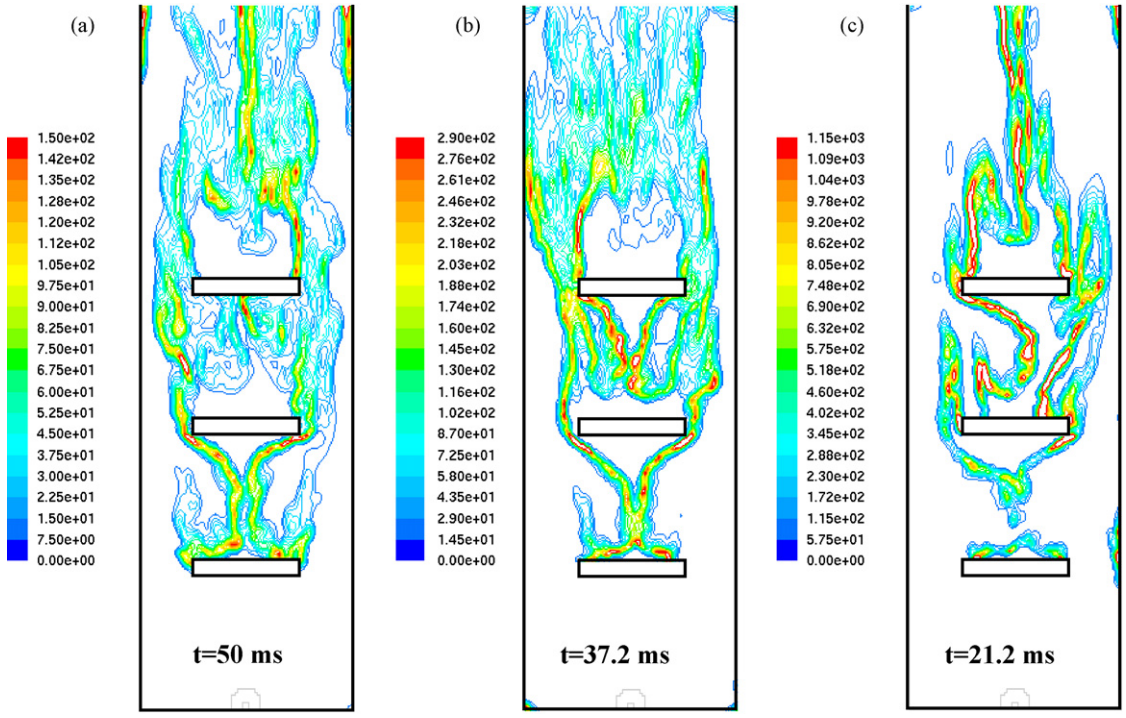

Fig. 5. Field profiles of the sgs combustion rate [kg/m^3 s] as computed for different combustion models: (a) Colin et al. [9]; (b) Charlette et al. [12]; (c) Pitsch and Duchamp de Lageneste [13]. (The profiles were taken at the central plane of the explosion chamber).

Table 3
Original (literature) and *adjusted* (present work) values of constants and parameters for each sgs combustion model tested.

Sgs combustion model	Constants and parameters for steady flame propagation (literature)	Constants and parameters for unsteady flame propagation (present work)
Colin et al. [9]	$\beta = 1$	$\beta = 9$
Flohr and Pitsch [10]	$a = 0.52$	$a = 0.16$
Kim and Menon [11]	$\beta = 1$; $\gamma = 2$; $A = 6$; $c_v = 0.05$	$\beta = 0.1$; $\gamma = 2$; $A = 3.8$; $c_v = 0.05$
Charlette et al. [12]	$\beta = 0.5$	$\beta = 0.5$
Pitsch and Duchamp de Lageneste [13]	$b_1 = 2$; $b_3 = 1$	$b_1 = 0.24$; $b_3 = 1$

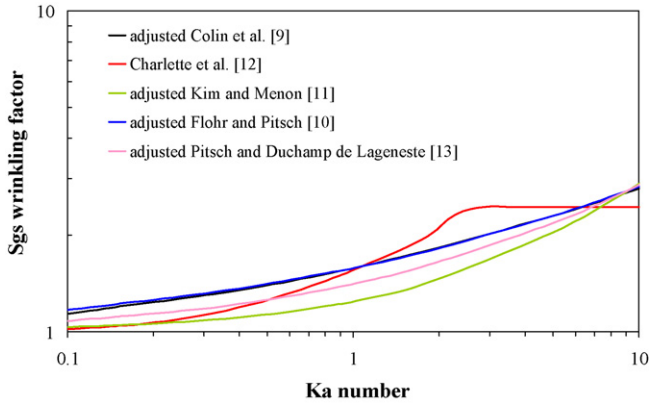

Fig. 6. Sgs wrinkling factor *versus* the Ka number for the *adjusted* combustion models.

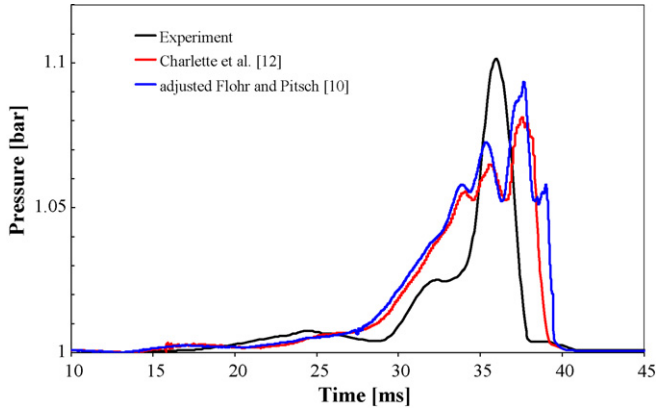

Fig. 8. Pressure time history at the bottom end of the explosion chamber: experimental data by Patel et al. [25] and LES results as obtained with the sgs combustion model by Charlette et al. [12] and the *adjusted* sgs combustion model by Flohr and Pitsch [10].

As an example of the results obtained with the *adjusted* sgs combustion models, Figs. 7 and 8 show the comparison between the experimental data for flame speed profile and pressure time history and the corresponding LES predictions as found using the *adjusted* model by Flohr and Pitsch [10]. The results by Charlette et al. [12] are also reported in these figures.

As found with Charlette et al. [12], the *adjusted* model reproduces well the experimental flame speed profile and, although the structure of the pressure curve is different from the experiment, it gives good predictions for both maximum pressure and corresponding time. Similar good agreement for flame speed and pressure peak is also found with the *adjusted* sgs models other than Flohr and Pitsch [9,11,13].

This confirms that the differences in the predictive capability of the original (not *adjusted*) sgs combustion models [9–11,13] and the sgs model by Charlette et al. [12] depend on the quantitative differences in the trends of Fig. 2.

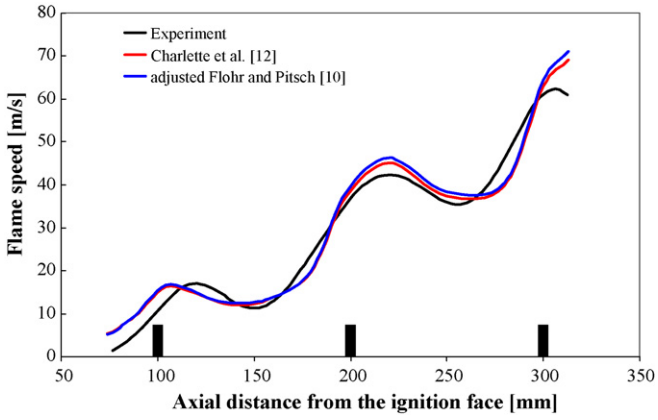

Fig. 7. Flame speed *versus* the axial distance from the ignition face: experimental data by Patel et al. [25] and LES results as obtained with the sgs combustion model by Charlette et al. [12] and the *adjusted* sgs combustion model by Flohr and Pitsch [10].

5. Conclusions

An assessment of different sub-grid scale (sgs) combustion models proposed for large eddy simulation (LES) of steady turbulent premixed combustion [9–13] has been performed to identify the model that best predicts unsteady flame propagation through obstacles. Numerical results have been compared to the experimental data by Patel et al. [25] for premixed deflagrating flame in a vented chamber initially filled with a quiescent mixture of stoichiometric methane and air. The chamber contains three sequential obstacles that ensure the full development of turbulent combustion.

It is shown that all sgs combustion models are able to reproduce qualitatively the experiment in terms of step of flame acceleration and deceleration around each obstacle, and shape of the propagating flame. Without adjusting any constants and parameters, the sgs model by Charlette et al. [12] also provides satisfactory quantitative predictions for flame speed and pressure peak (maximum pressure and corresponding time). Conversely, the sgs combustion models other than Charlette et al. [9–11,13] give correct predictions only after an *ad hoc* tuning of constants and parameters.

Acknowledgements

The authors thank Vincenzo Smiglio for his technical assistance in the computing activity. This work was partially funded by the research project “MAP-Gas Naturale”.

References

[1] V. Di Sarli, A. Di Benedetto, E. Salzano, G. Ferrara, G. Russo, Mitigation of gas explosions in industrial equipment by means of venting systems, in: P.B. Warey (Ed.), New Research on Hazardous Materials, Nova Science Publishers, New York, 2007, pp. 249–291.
[2] A. Di Benedetto, V. Di Sarli, Theory, modeling and computation of gas explosion phenomena, in: M. Lackner, F. Winter, A.K. Agarwal (Eds.), Handbook of Com-

bustion vol. 3: Gaseous and Liquid Fuels, Wiley-VCH Books, Wiley-VCH Verlag GmbH & Co. KGaA, Weinheim, 2010, pp. 49–74.
[3] T. Poinsot, D. Veynante, Theoretical and Numerical Combustion, 2nd ed., R.T. Edwards, Philadelphia, 2005.
[4] H. Pitsch, Large-eddy simulation of turbulent combustion, Annu. Rev. Fluid Mech. 38 (2006) 453–482.
[5] M. Boger, D. Veynante, H. Boughanem, A. Trouvé, Direct numerical simulation analysis of flame surface density concept for large eddy simulation of turbulent premixed combustion, in: Proc. 27th Int. Symp. on Combustion, The Combustion Institute, 1998, pp. 917–925.
[6] H.G. Weller, G. Tabor, A.D. Gosman, C. Fureby, Application of a flame-wrinkling LES combustion model to a turbulent mixing layer, in: Proc. 27th Int. Symp. on Combustion, The Combustion Institute, 1998, pp. 899–907.
[7] W.-W. Kim, S. Menon, H.C. Mongia, Large-eddy simulation of a gas turbine combustor flow, Combust. Sci. Technol. 143 (1999) 25–62.
[8] M. Boger, D. Veynante, Large eddy simulations of a turbulent premixed V-shape flame, in: C. Dopazo et al. (Eds.), Advances in Turbulence VIII, Proc. 8th European Turbulence Conference, 2000, pp. 449–452.
[9] O. Colin, F. Ducros, D. Veynante, T. Poinsot, A thickened flame model for large eddy simulations of turbulent premixed combustion, Phys. Fluids 12 (2000) 1843–1863.
[10] P. Flohr, H. Pitsch, A turbulent flame speed closure model for LES of industrial burner flows, in: Proc. CTR Summer Program, 2000, pp. 61–82.
[11] W.-W. Kim, S. Menon, Numerical modeling of turbulent premixed flames in the thin-reaction-zones regime, Combust. Sci. Technol. 160 (2000) 119–150.
[12] F. Charlette, C. Meneveau, D. Veynante, A power-law flame wrinkling model for LES of premixed turbulent combustion. Part I. Non-dynamic formulation and initial tests, Combust. Flame 131 (2002) 159–180.
[13] H. Pitsch, L. Duchamp de Lageneste, Large-eddy simulation of premixed turbulent combustion using a level-set approach, Proc. Combust. Inst. 29 (2002) 2001–2008.
[14] Y. Huang, H.-G. Sung, S.-Y. Hsieh, V. Yang, Large-eddy simulation of combustion dynamics of lean-premixed swirl-stabilized combustor, J. Propul. Power 19 (2003) 782–794.
[15] R. Knikker, D. Veynante, C. Meneveau, A dynamic flame surface density model for large eddy simulation of turbulent premixed combustion, Phys. Fluids 16 (2004) L91–L94.
[16] S. Roux, G. Lartigue, T. Poinsot, U. Meier, C. Bérat, Studies of mean and unsteady flow in a swirled combustor using experiments, acoustic analysis, and large eddy simulations, Combust. Flame 141 (2005) 40–54.
[17] G. Boudier, L.Y.M. Gicquel, T. Poinsot, D. Bissières, C. Bérat, Comparison of LES, RANS and experiments in an aeronautical gas turbine combustion chamber, Proc. Combust. Inst. 31 (2007) 3075–3082.
[18] G. Staffelbach, L.Y.M. Gicquel, G. Boudier, T. Poinsot, Large eddy simulation of self excited azimuthal modes in annular combustors, Proc. Combust. Inst. 32 (2009) 2909–2916.
[19] M.P. Kirkpatrick, S.W. Armfield, A.R. Masri, S.S. Ibrahim, Large eddy simulation of a propagating turbulent premixed flame, Flow Turbul. Combust. 70 (2003) 1–19.
[20] A.R. Masri, S.S. Ibrahim, B.J. Cadwallader, Measurements and large eddy simulation of propagating premixed flames, Exp. Therm. Fluid Sci. 30 (2006) 687–702.
[21] S.R. Gubba, S.S. Ibrahim, W. Malalasekera, A.R. Masri, LES modeling of premixed deflagrating flames in a small-scale vented explosion chamber with a series of solid obstructions, Combust. Sci. Technol. 180 (2008) 1936–1955.
[22] V. Di Sarli, A. Di Benedetto, G. Russo, S. Jarvis, E.J. Long, G.K. Hargrave, Large eddy simulation and PIV measurements of unsteady premixed flames accelerated by obstacles, Flow Turbul. Combust. 83 (2009) 227–250.
[23] V. Di Sarli, A. Di Benedetto, G. Russo, Using large eddy simulation for understanding vented gas explosions in the presence of obstacles, J. Hazard. Mater. 169 (2009) 435–442.
[24] S.S. Ibrahim, S.R. Gubba, A.R. Masri, W. Malalasekera, Calculations of explosion deflagrating flames using a dynamic flame surface density model, J. Loss Prev. Process Ind. 22 (2009) 258–264.
[25] S.N.D.H. Patel, S. Jarvis, S.S. Ibrahim, G.K. Hargrave, An experimental and numerical investigation of premixed flame deflagration in a semiconfined explosion chamber, Proc. Combust. Inst. 29 (2002) 1849–1854.
[26] P.A. Libby, F.A. Williams (Eds.), Turbulent Reacting Flows, Academic Press, London, 1994.
[27] D.K. Lilly, A proposed modification of the Germano subgrid-scale closure method, Phys. Fluids A 4 (1992) 633–635.
[28] L.G. Loitsyanskiy, Mechanics of Liquids and Gases, sixth ed., Begell House, New York, 1995.
[29] A. Trouvé, T. Poinsot, The evolution equation for the flame surface density in turbulent premixed combustion, J. Fluid Mech. 278 (1994) 1–31.
[30] W.-W. Kim, S. Menon, Application of the localized dynamic subgrid-scale model to turbulent wall-bounded flows, Technical Report AIAA-97-0210, American Institute of Aeronautics and Astronautics, 35th Aerospace Sciences Meeting & Exhibit, Reno, 1997.
[31] R.G. Abdel-Gayed, D. Bradley, A two-eddy theory of premixed turbulent flame propagation, Philos. Trans. R. Soc. Lond. Ser. A 301 (1981) 1–25.
[32] V.L. Zimont, A.N. Lipatnikov, A numerical model of premixed turbulent combustion of gases, Chem. Phys. Reports 14 (1995) 993–1025.
[33] N. Peters, The turbulent burning velocity for large-scale and small-scale turbulence, J. Fluid Mech. 384 (1999) 107–132.
[34] A. Pocheau, Scale invariance in turbulent front propagation, Phys. Rev. E 49 (1994) 1109–1122.
[35] V. Yakhot, Propagation velocity of premixed turbulent flames, Combust. Sci. Technol. 60 (1988) 191–214.
[36] B.A. Kader, Temperature and concentration profiles in fully turbulent boundary layers, Int. J. Heat Mass Transfer 24 (1981) 1541–1544.
[37] G. Yu, C.K. Law, C.K. Wu, Laminar flame speeds of hydrocarbon + air mixtures with hydrogen addition, Combust. Flame 63 (1986) 339–347.
[38] V. Di Sarli, A. Di Benedetto, Laminar burning velocity of hydrogen-methane/air premixed flames, Int. J. Hydrogen Energy 32 (2007) 637–646.
[39] Fluent 6.3.26, Fluent Inc., Lebanon, NH, USA, website: www.fluent.com, 2007 (accessed 18.07.09).